PHOTOCATALYTIC HYDROGEN GENERATION FROM SEAWATER USING HIGH-PERFORMANCE POLYMERIC MATERIALS

An Undergraduate Research Scholars Thesis

by

GHALYA ABDULLA[1] AND NOORA AL-SUBAIEI[2]

Submitted to the LAUNCH: Undergraduate Research office at
Texas A&M University
in partial fulfillment of requirements for the designation as an

UNDERGRADUATE RESEARCH SCHOLAR

Approved by
Faculty Research Advisors: Dr. Mohammed Al-Hashimi
Dr. Konstantinos E. Kakosimos

May 2022

Majors: Chemical Engineering[1,2]

RESEARCH COMPLIANCE CERTIFICATION

Research activities involving the use of human subjects, vertebrate animals, and/or biohazards must be reviewed and approved by the appropriate Texas A&M University regulatory research committee (i.e., IRB, IACUC, IBC) before the activity can commence. This requirement applies to activities conducted at Texas A&M and to activities conducted at non-Texas A&M facilities or institutions. In both cases, students are responsible for working with the relevant Texas A&M research compliance program to ensure and document that all Texas A&M compliance obligations are met before the study begins.

We, Ghalya Abdulla[1] and Noora Al-Subaiei[2], certify that all research compliance requirements related to this Undergraduate Research Scholars thesis have been addressed with our Research Faculty Advisors prior to the collection of any data used in this final thesis submission.

This project did not require approval from the Texas A&M University Research Compliance & Biosafety office.

TABLE OF CONTENTS

ABSTRACT

Photocatalytic Hydrogen Generation from Seawater using High-Performance Polymeric Materials

Ghalya Abdulla[1] and Noora Al-Subaiei[2]
Department of Chemical Engineering[1,2]
Texas A&M University

Research Faculty Advisor: Dr. Mohammed Al-Hashimi
Department of Chemistry
Texas A&M University

Research Faculty Advisor: Dr. Konstantinos E. Kakosimos
Department of Chemical Engineering
Texas A&M University

Recently, there has been renewed interest in the use of solar energy as a resource to meet the world's energy needs in an environmentally sustainable way. Hence, our research focuses on the generation of hydrogen from non-fresh water using the sun as an energy source. The research aims to characterize, assess, and developed new research-grade materials and commercial photocatalysts that can achieve sunlight-driven unassisted photo-splitting of water. In this work, novel conjugated polymer nanoparticles were developed and characterized. The nanoparticles are composed of a donor-acceptor system where two acceptors (**A1** and **A2**) were developed and tested, and different ratios of each donor-acceptor system were assessed. The use of platinum or molybdenum as co-catalysts was explored. Hydrogen evolution reactions with ascorbic acid as sacrificial reagent was performed using these materials and their performance was assessed. The

results show that the first system consisting of acceptor **A1** and the donor (**A1/D**) produces more hydrogen than the (**A2/D**) system. Furthermore, the best ratio of donor to acceptor was determined to be 10:90 for the (**A1/D**) system. The use of platinum as a co-catalyst was shown to result in a better performance in terms of hydrogen production compared to the use of molybdenum. Furthermore, the results show that the use of nanoparticles suspended in solution results in a higher hydrogen evolution rate compared to the use of films. Hydrogen production of 2018 micromole per hour of catalyst was achieved using the **A1/D** nanoparticle system with platinum, which represents the best result as initial findings. For future steps, optimization of the reaction will take place to generate more hydrogen.

ACKNOWLEDGEMENTS

Contributors

We would first like to thank our supervisors, Professors Mohammed Al-Hashimi and Konstantinos Kakosimos, whose expertise was invaluable in formulating the strategy of our work. All their efforts, guidance, and time they provided us to learn the basics of research to successfully achieve the project tasks within the time frame. We believe that their insightful feedback had pushed our research to a higher level.

In the end, we would like to thank the undergraduate students, Malek Helali, Hanan Al-Ansari, Ibrahim Al-Baker, and Rowan Abdulgadir for their valuable contribution and working with us in the initial UREP project, which we were able to work with more acceptor and surfactant samples to study and produce this thesis precisely with the best outcomes.

Funding Sources

We would also like to thank Qatar National Research Fund (QNRF) and the National Priorities Research Program, for the grant they provided to support the research project under the Undergraduate Research Experience Program (UREP); with a grant ID of [UREP25-095-1-014]. In addition, thanks to Dr. Dhruv Arora from Qatar Shell who had provided huge efforts to support us by engaging with our research work and promoting us to enhance our technical skills.

NOMENCLATURE

EPA	Environmental Protection Agency GHG Green House Gas
D/A	Donor/Acceptor
XRD	X-ray diffraction
SEM	Scanning Electron Microscopy
TEM	Transmission Electron Microscopy
HER	Hydrogen Evolution Reaction
NMR	Nuclear Magnetic Resonance
UV-Vis	Ultraviolet Visible
GC	Gas Chromatography
SMA	Small Molecule Acceptor
DP	Donor Polymer
SDS	Sodium Dodecyl Sulfate
NPS	Nanoparticle Precursor Solutions
TAMUQ	Texas A&M University at Qatar
QNRF	Qatar National Research Fund

1. INTRODUCTION

The energy crises and environmental pollution are major challenges in the development of our ecosystems and greatly impede the sustainable development of mankind.[1] Widely available and abundant solar energy is an important renewable resource to meet the world's environmentally sustainable energy needs. However, due to solar irregularities, cost-effective energy storage is a prerequisite for bringing greater solar efficiency to the energy market.[2] Ultimately, the combination of hydro and solar power represents an attractive and essentially viable solution to our energy needs as presented in *Figure* 1.1. [3-8]

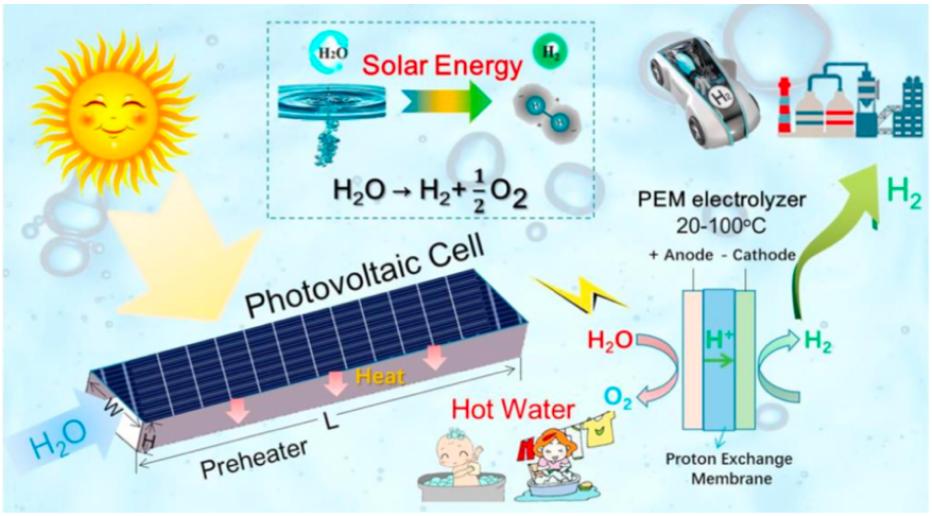

Figure 1.1: Shows the combination of solar energy storage and water through hydrogen evolution system [9]

Based on recent studies conducted in the United States by Environmental Protection Agency (EPA), data had shown a continuous increase in Greenhouse gas (GHG) emissions due to three major sources. Transportation, electricity, and the combustion of fossil fuels in industries as shown in *Figure* 1.2.[1] The major contributes to the global increase of Green House Gas (GHG) emissions are both economic and population growth.

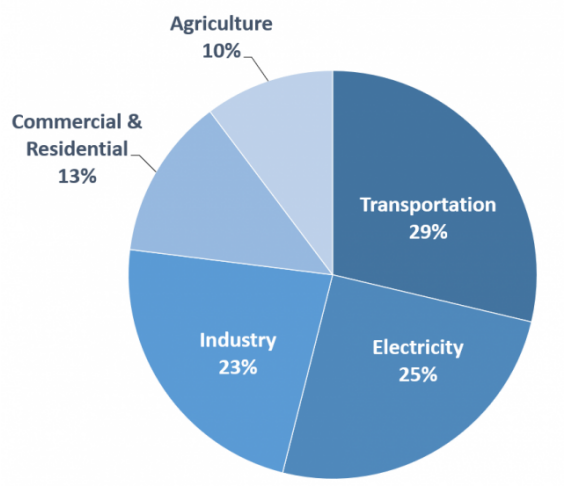

Figure 1.2: Shows the percentage of Green House Gas (GHG) emission in the US in 2019 adapted from EPA [1]

A long-term sustainable goal that's set by the European Union to be achieved by 2050 is to cut 80-95% of Greenhouse gas emissions. Hence, Hydrogen contributes a long-term solution to reduce the emission of Greenhouse gases in the environmental, economic, and industrial sectors in energy production.[2] Japan had also promoted hydrogen energy development worldwide in order to set up 10,000 hydrogen refueling stations within 10 years.[3] Hence, this will act as a solution for the major issue of the increase of GHG which is Transportation.[1] Moreover, Japan adopted a long-term strategy to reduce emissions under Paris Agreement which includes the goal for the country to become carbon-neutral by 2050. Hence, this will cut off the emission of (GHG) by more than half.[3] Therefore, this acts as proof that hydrogen gas will play a key role in an environmentally sustainable energy cycle.

1.1 Objective

Hydrogen can be produced via various processes, for example, water electrolysis, natural gas reforming processes, coal gasification, natural gas reforming processes, biomass pyrolysis, and dark fermentation process. Hence, our research focuses on the generation of hydrogen from non-fresh water using the sun as an energy source. The research aims to characterize. In addition,

assess the developed versatile strategy, based on interfacing 2D nano-sheets of existing semiconductors with 1D π-conjugated polymers, to systematically modulate the edge electronic structure of the nano-sheets and to allow for photosensitization of the hydrogen evolution reaction. Hence, developed new research-grade materials and commercial photo catalysts that can achieve sunlight-driven unassisted photo-splitting of water.

1.2 Conjugated Polymers

The conjugated polymers and covalent organic frameworks have been the most attractive materials for hydrogen evolution. This is because their molecular structures can be precisely controlled from their physical properties and energy levels.[10-12] Nonetheless, the external quantum efficiencies of these photocatalysts have been restricted by huge exciton energy binding and small exciton diffusion lengths of organic semi-conductors.[13] This can result in higher rates of exciton in the semi-conductors, and thus ineffective charges generation can occur which will affect the photocatalyst surface in the redox reaction.[14] To control this restriction, most research suggested increasing the interfacial area of the semi-conductor or electrolyte through nanoparticle formation to enhance the exciton dissociation. To be more specific, prepare donor/acceptor (D/A) semi-conductor heterojunction that will help in exciton dissociation at the photocatalyst interface.[15, 16] The fabrication of conjugated polymer nanoparticles can be easily achieved through (D/A) heterojunction in which (D/A) semiconductors are mixed using the same nanoparticle.[17] However, this feature has not been implemented yet, since most recent studies concentrate on testing the photocatalytic performance of hydrogen evolution photocatalysts produced through a single conjugated polymer.[18-20]

Recent research has developed an experimental procedure of organic nanoparticles fabrication by incorporating with (D/A) heterojunction, which leads to improving the

photocatalytic hydrogen evolution compared to the single-component nanoparticles method. The nanoparticles were manufactured through a mini-emulsion process, and sodium dodecyl sulfate (SDS) was used as stabilizing surfactant. The donor polymer used was (PTB7-Th) combined with the acceptor (EH-IDTBR) as shown in *Figure* 1.3. In addition, the co-catalyst used for nanoparticles fabrication was Platinum.[21]

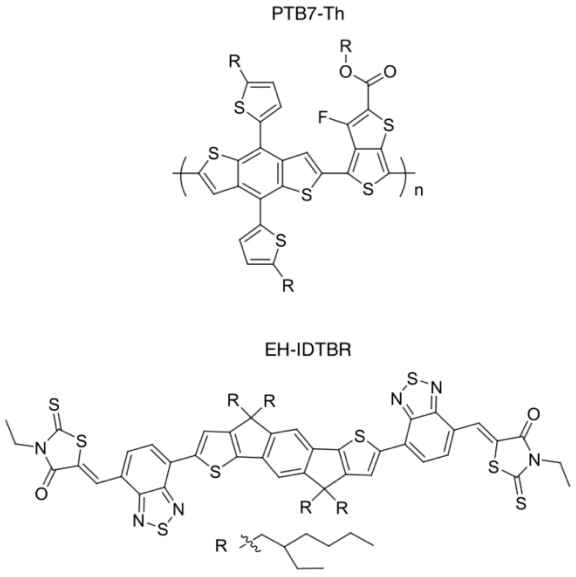

Figure 1.3: Shows the combination of the donor (PTB7-Th) and acceptor (EH-IDTBR) [21]

1.3 Methodology

This paper focused on conducting an experimental procedure for nanoparticle fabrication and hydrogen evolution. The nanoparticles are composed of a donor and a non-fullerene fused-ring electron acceptor (NF-FREA) system where three acceptor-donor systems (NF-FREA1/D, NF-FREA2/D, NF-FREA3/D). The experimental procedure was accomplished by preparing different ratios of donor and acceptor in chloroform, heating the mixture overnight, preparing the nanoparticle precursor solution, sonicating the mixture through an ultrasonic device, and finally, the mixture goes to dispersion filtration. Moreover, the hydrogen evolution was achieved using a

solar simulator. The operational conditions of hydrogen evolution were temperature of 40 ºC, 0.2 M ascorbic acid, 100 rpm stirring rate, and 10 ml of water. The errors that might affect the results could be through injecting impure hydrogen or gas leak in the reactor.

1.4 Characterization

In this work, different compound characterization was implemented such as Nuclear Magnetic Resonance (NMR), Ultraviolet-visible spectroscopy (UV-Vis), and gas chromatography. The chemical kinetics of hydrogen was studied via photochemically and electrochemically driven water splitting, of distilled water, using the selected catalysts. The locally sourced water, seawater, and industrial feeds will be used to assess the performance of each catalyst against the reference which is the distilled water. The identification of the byproducts in the chemical reaction will be achieved by the combination of gas and liquid phase analytical methods.

2. METHOD

A combination of sequential and parallel tasks was carried out to accomplish the objectives of this proposal, in a synergistic manner drawing on the expertise of the 3 different nanoparticles configuration which were (**A1/D**), (**A2/D**), and (**A3/D**). We have quickly converged on promising hybrid architectures and are further optimizing the materials' catalytic activity based on fundamental mechanistic understanding and the development of structure-functional relationships. Moreover, the objective was accomplished by starting with stock solution preparations in which donors and acceptors were mixed using sodium dodecyl sulfate (SDS) as a surfactant to stabilize the mixture. The PTFE filter was one of the techniques used to filter the mixture and its diameter was chosen to be (0.45 μm) and this was based on the molecular weight of the chemical. The higher the molecular weight, the bigger diameter that was required. At this point, nanoparticle fabrication was carried out by mixing the stock solution with the desired ratio of the nanoparticle composition. Furthermore, one of the methods used was the sonication process, where the mixture has been sonicated for a while to ensure uniform mixing of the mixture and break the microemulsion that was formed from nanoparticle precursor solution. Hydrogen evolution reactions were also performed in the photoreactor to identify the performance of the acceptor and donor system. During the hydrogen evolution reactions, different catalysts have been tested out such as platinum and molybdenum. In addition, other characterizations were achieved such as NMR and UV-VIS. The NMR was implemented to identify the functional groups present in the donor and acceptor molecule, while the UV-VIS was used to determine the amount of energy of film and solution nanoparticles.

3. RESULTS

3.1 Synthetic Pathway

Small Molecule Acceptor (SMA) and Donor Polymer (DP) nanoparticles were synthesized as depicted in *Figure 3.1*. The (SMA) was formed by reacting EH-IDTBR with $Pd(PPh_3)_4$ and toluene. Then, a compound produced having 1480.22 g/mol molecular weight and a 3-Butyl-2-Thio-4-Thiazolidinone was added to it under piperidine and chloroform conditions as shown in *Figure 3.1*. However, the (DP) was higher in molecular weight compared to SMA, therefore it can be observed that DP absorbs more light. Note that three different acceptors were tested as shown in *Figure* 3.2*, Figure 3.3,* and *Figure* 3.4.

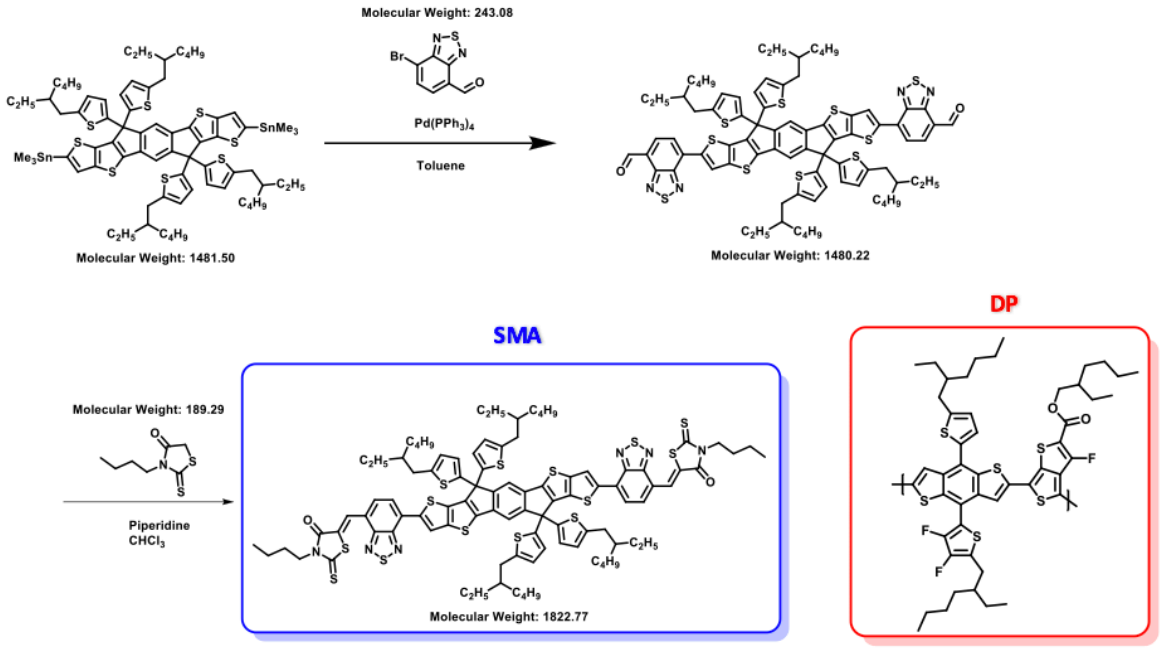

Figure 3.1: The Synthesis of Small Molecule Acceptor (SMA) and Donor Polymer (DP) Nanoparticle which was digitally drawn via chem drew software

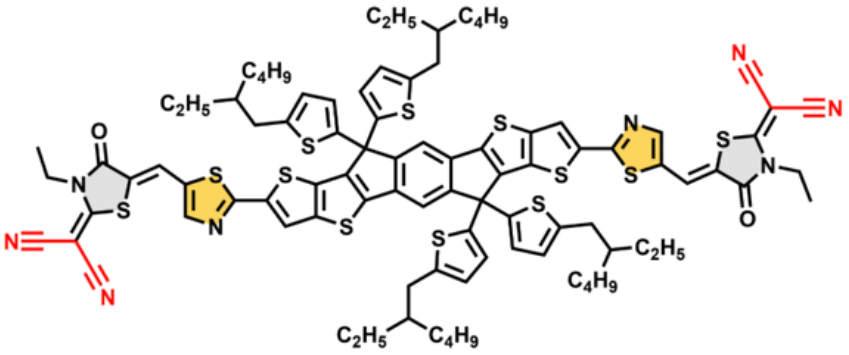

Figure 3.2: Shows Acceptor 1 (A1) which was digitally drawn via ChemDraw software

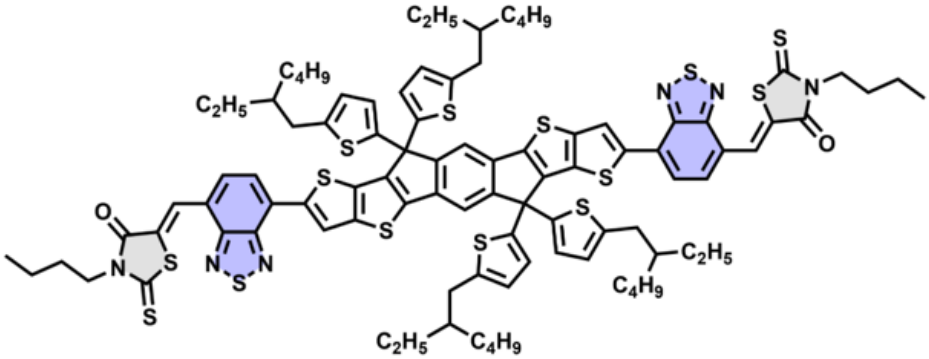

Figure 3.3: Shows Acceptor 2 (A2) which was digitally drawn via ChemDraw software

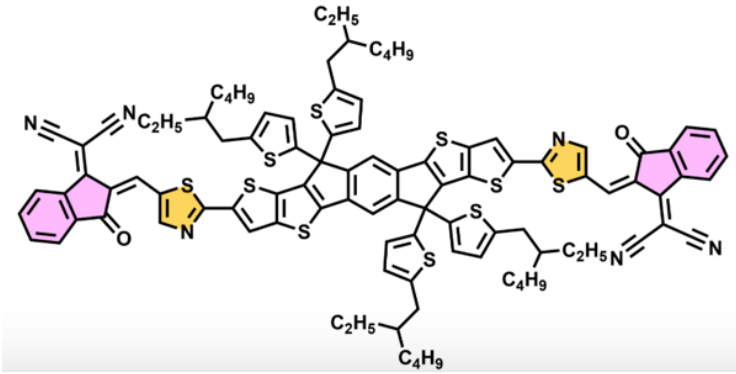

Figure 3.4: Shows Acceptor 3 (A3) which was digitally drawn via ChemDraw software

3.2 Chemical Preparations

The nanoparticle fabrication was done by preparing individual stock solutions (0.5 mg/mL) of the donor and acceptor in chloroform. The donor and acceptor were mixed (25 mg and 50 mg/mL) and using sodium dodecyl sulfate (SDS) as stabilizing surfactant as presented in *Figure* 3.5. Those donors and acceptors (D/A) were chosen due to their strong light absorption. The mixture was heated overnight under 80^{o}C conditions to ensure a full dissolution and was then filtered using PTFE filters. The filter diameter was chosen based on the molecular weight of the compound. The higher the molecular weight, the bigger diameter was required. An error may occur if a small diameter was chosen for the high molecular compound since the solution will not move freely and stick on the tube resulting in an inaccurate desired ratio. Therefore, a 0.45 μm-PTFE filter was used to filter the donor stock solution and a 0.2 μm-PTFE filter for the acceptor. The preparation of the Nanoparticle Precursor Solutions (NPS) was done by using the stock solution and mixing them in terms of the desired ratio of the nanoparticle composition, as shown in *Table 3.1,* to produce a total of 5 mL of the precursor solution for each composition. Finally, the solutions were slowly injected into 10 mL of 0.5wt% of sodium dodecyl sulfate each. Then, the whole mixture was stirred vigorously (at 1500 rpm) for 15 minutes at 45^{o}C and resulted a colorless solution as shown in *Figure* 3.6. The stirrer rate was high due to the large size of nanoparticles. This resulted in the formation of a pre-emulsion.

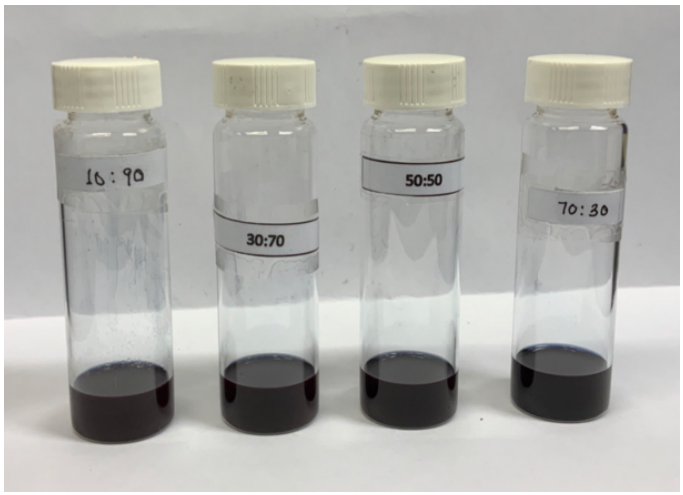

Figure 3.5: Donor and acceptor mixture with different ratios (taken at TAMUQ, Lab 361E)

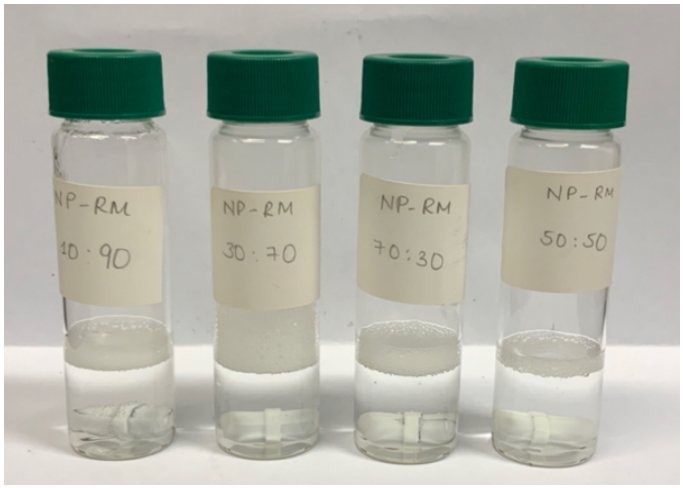

Figure 3.6: NPS with different ratios (taken at TAMUQ, Lab 361E)

Table 3.1: Nanoparticles Precursor Solutions Preparation in Different Ratios

Donor/Acceptor	Donor (0.5 mg/mL)	Acceptor (0.5 mg/mL)	Final Volume (mL)
10%	0.5	4.5	5
30%	1.5	3.5	5
50%	2.5	2.5	5
70%	3.5	1.5	5
Total Volume (mL)	8.75 mL ~ 10 mL	16.25 mL ~ 10 mL	-

The sonication process of the mixtures was done using the ultrasonic processor. The mixtures have been sonicated for either approximately 15 minutes or until the mixtures were uniformly mixed and no white lines were formed in the mixture during sonication. These white lines indicate the breaking of the microemulsion. The purpose of performing this step was to break the microemulsion that has been formed in the nanoparticle precursor solution perpetration step and to create a mini emulsion. In addition, an observation was done during the process, which was the mixture forming into two layers, one layer representing the chloroform which has dark purple color whereas the second layer representing the nanoparticles, and they were colored in light purple. *Figure* 3.7 shows an example of a mixture before and after the sonication process. After the sonication process, the mixtures were heated to 85 °C in order to remove the chloroform from the mixture. Following this, a dispersion filtration was done for the mixtures using a 0.45 mm PTFE filter in order to remove any large aggregates or debris from the precursor tip. *Figure* 3.8 shows the mixtures after filtration. This concluded the nanoparticle fabrication.

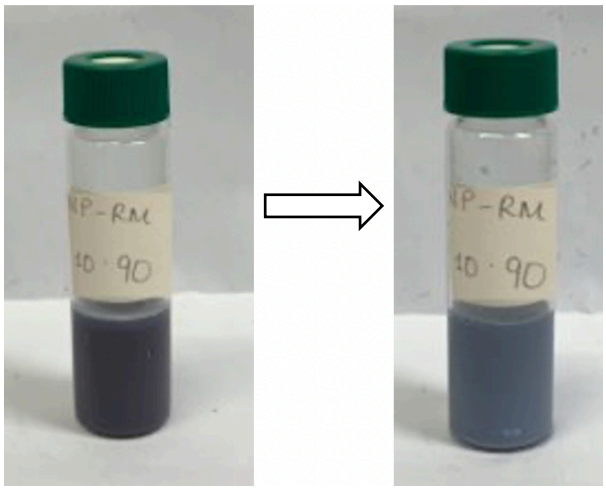

Figure 3.7: Mixture before and after sonication process (taken at TAMUQ, Lab 361E)

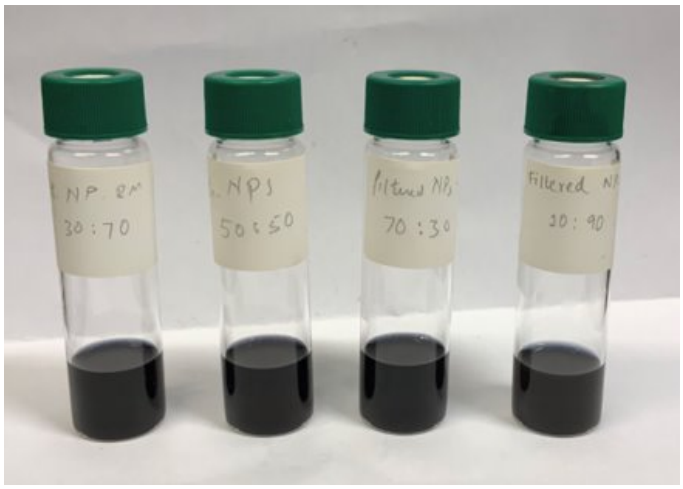

Figure 3.8: Mixtures after filtration (taken at TAMUQ, Lab 361E)

3.3 Hydrogen Evolution Reaction

To determine the performance of the acceptor-donor systems, hydrogen evolution reactions were performed in a photoreactor, and the amount of hydrogen produced was measured. 20 mL of 0.2 M ascorbic acid in deionized water was used as the sacrificial electron donor during the reaction. The use of two co-catalysts was explored – platinum and molybdenum. This was done by adding 1 mL of either a potassium hexachloroplatinate solution or molybdenum disulphide solution as the platinum and molybdenum sources respectively. The reaction mixture was then transferred into the reactor and stirred slowly. Prior to starting the reaction, the reactor was first purged with Argon gas. The solar simulator was then started, and a calibration hydrogen injection was first performed. The reaction was then allowed to proceed, and the hydrogen evolution was monitored using a gas chromatograph. The reactions were mainly performed in batches.

3.4 Characterization

The stability and degradability of the catalyst were further explored through long-term, cyclical experimental procedures and analytical methods such as X-Ray Diffraction (XRD), Scanning Electron Microscopy (SEM), and Transmission Electron Microscopy (TEM). Finally, the hydrogen evolution percentage was obtained using a solar simulator device. However, prior to conducting the hydrogen evolution reaction, the nanoparticles and the donor and acceptor molecules were characterized. NMR spectroscopy was conducted for the donor and acceptor molecules that were used in nanoparticle fabrication. The purpose of NMR was to determine the functional groups present in the donor and acceptor molecule. The solvent that was used as a background for the NMR was $CDCl_3$ is the chloroform. *Figure 3.9* and *Figure 3.10* show the results of the NMR spectroscopy.

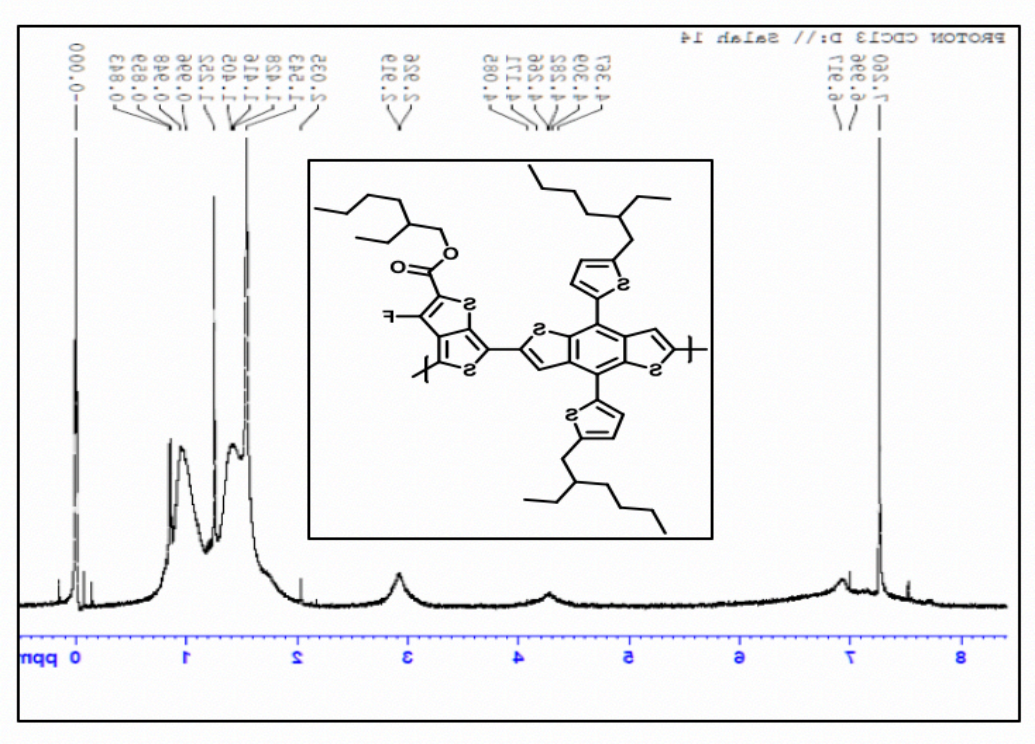

Figure 3.9: Illustrates the NMR-Donor molecule (taken at TAMUQ, Lab 118A)

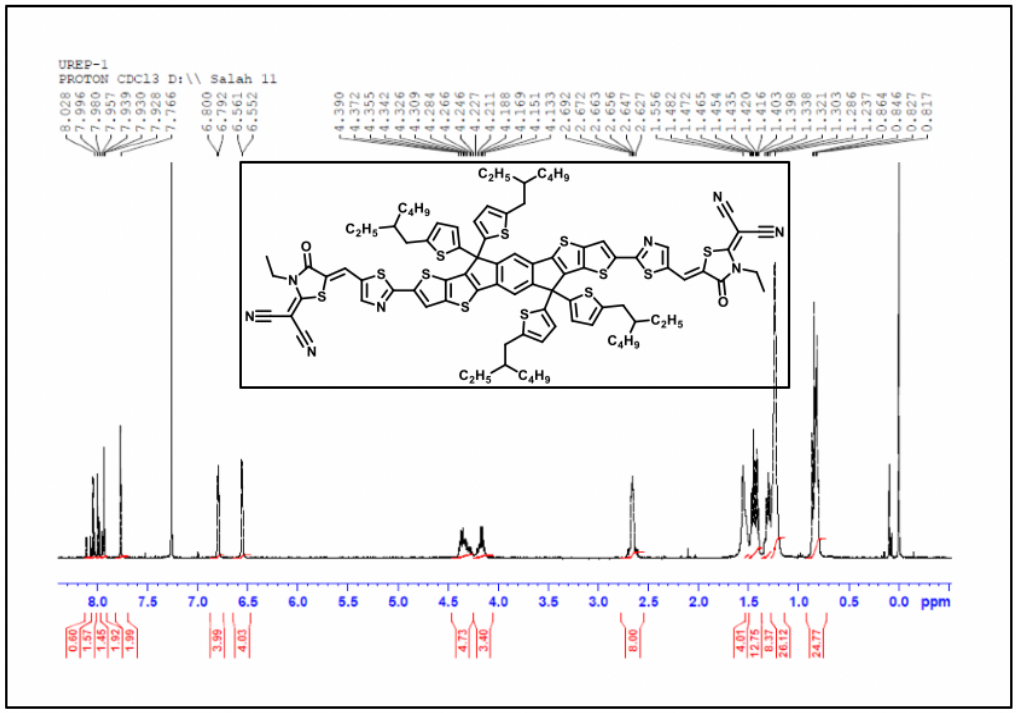

Figure 3.10:Illustrates NMR-Acceptor Molecule (taken at TAMUQ, Lab 118A)

UV Spectroscopy was conducted for the different ratios of the nanoparticle solutions as well as the pure donor and acceptor solutions. The solvent used for the nanoparticle solutions was dissolved in SDS. Hence prior to obtaining their absorption spectra, a background run was performed using two samples containing SDS. This was also done using chloroform since it was the solvent used for the pure donor and acceptor stock solutions. *Figure 3.11* shows the UV-VIS machine that was used, and *Figure 3.12* shows the absorption spectra obtained for the various samples. While, *Table 3.2* shows the quantified band gap energies for solution and film acceptors and donors.

Figure 3.11: UV-VIS Machine (taken at TAMUQ, Lab 118A)

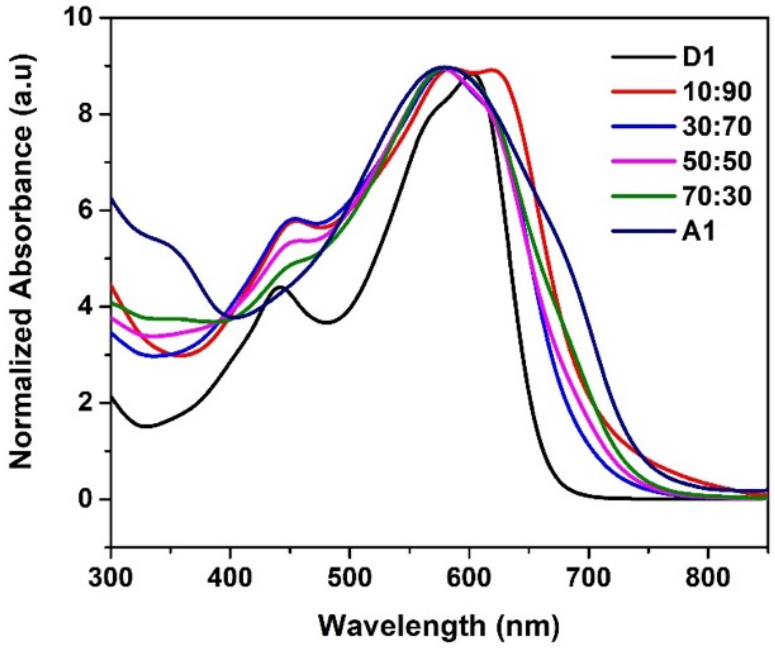

Figure 3.12: UV-Vis Absorption Spectra (taken at TAMUQ, Lab 118A)

Table 3.2: The band gap energy for solution and film acceptors and donors

Component	Wavelength(nm)	Energy(eV)
A1-Soln	638	1.944
A1-film	671	1.848
A2-Soln	685	1.810
A2-film	740	1.676
D1-Soln	717	1.729
D1-film	750	1.653

Referring to *Table 3.2,* the solution of acceptor 1 resulted in the highest energy production which was (1.944 eV) at 638 nm, while the energy film of acceptor 1 was (1.848 eV) at 671 nm. This proves that the solution of donors and acceptors has higher energies compared to films, this shows that the nanoparticle's solution had a smaller particles size. Thus, the solution of the nanoparticles would absorb light at a higher frequency and lower wavelength.

Following the nanoparticle fabrication and characterization, hydrogen evolution from the samples we prepared was measured in order to determine their photocatalytic activities. The Hydrogen Evolution Reaction (HER) involves the photocatalytic splitting of water to produce hydrogen. To conduct the HER, 2 mg of the 10:90 nanoparticle sample was mixed with 20 mL of 0.2 M ascorbic acid and 1 mL of 0.4 mg/mL of potassium hexachloroplatinate which acted as a co-catalyst. The reaction was conducted at 40 °C in a photoreactor as shown in *Figure 3.13*. A close up picture of organic catalyst nanoparticles in photocatalytic reactor is presented in *Figure 3.14*.

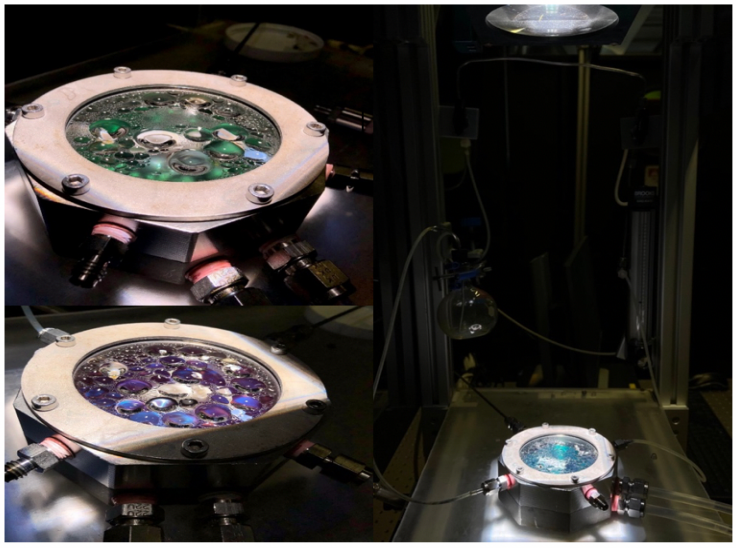

Figure 3.13: Photoreactor Setup (taken at TAMUQ, Lab 259F)

Figure 3.14: Close up of photocatalytic reactor containing a suspension of organic catalyst nanoparticles (taken by Malek Helali at TAMUQ, Lab 259F)

The photoreactor was connected to a GC-Mass spectrometer which identifies components of a sample and was essentially used to quantify the amount of hydrogen produced. The graph obtained from the spectrometer showed peaks corresponding to various components. The reactor was first purged with Argon to eliminate all dissolved oxygen from the system. Once the system was purged, 50 mL of hydrogen gas was injected for calibration. The changes in the

H_2 peak were observed and the experiment only started after the H_2 curve dropped back to its original background level. The solar simulator was turned on to begin the experiment, and the reaction mixture was stirred constantly at 200 rpm. The reaction was conducted in batch for three hours and the hydrogen production was measured every hour. The graph shown in *Figure 3.15* shows the peaks corresponding to the H_2 produced at each hour. The graph is later used to quantify the amount of hydrogen produced in mmol h^{-1} g^{-1}.

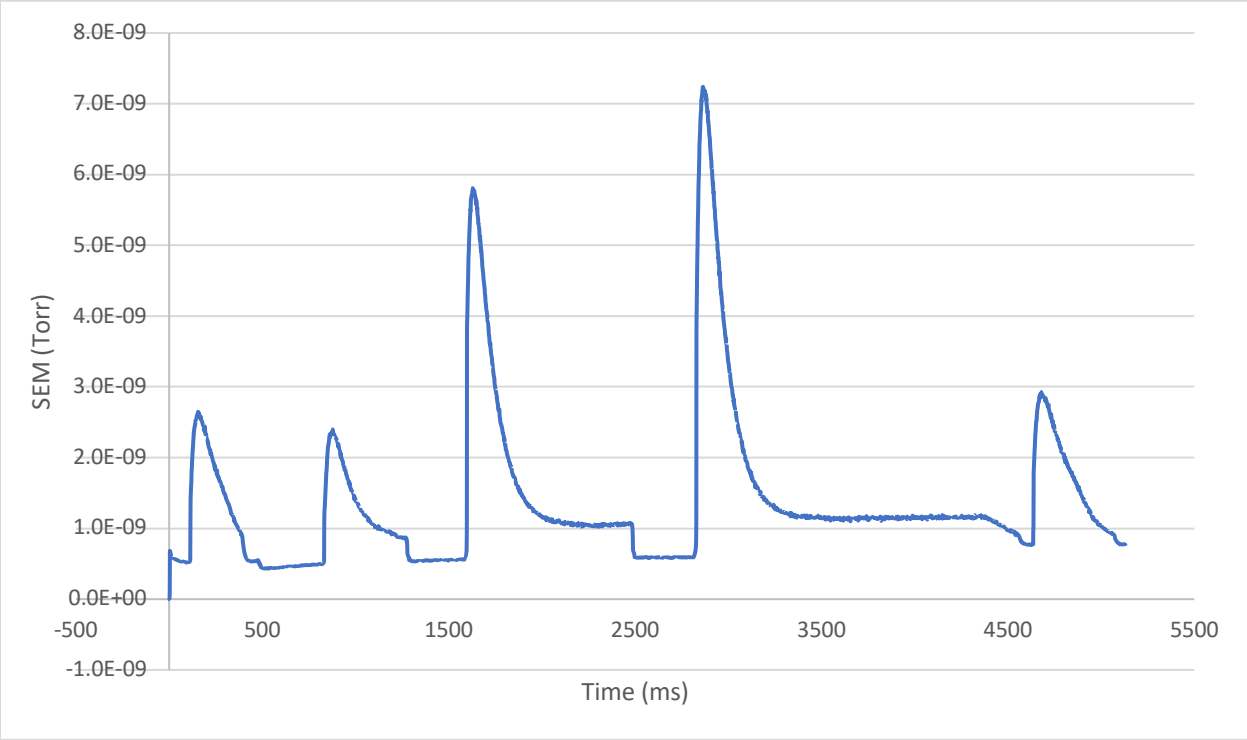

Figure 3.15: Shows the mass spectrum of H_2 peaks (taken at TAMUQ, Lab 259F)

Referring to *Figure 3.15*, the y-axis represents the pressure in Torr, while the x-axis shows the time in milliseconds. However, the first peak represents the injection of hydrogen in a continuous mode of operation. After three hours, three hydrogen peaks appeared, and the highest hydrogen evolution was observed after 3 hours from hydrogen injection. After three hours, the hydrogen production experienced a steady state and therefore hydrogen was injected at hour 5.

Two types of modes were used during the hydrogen evolution reaction Batch and Continuous mode. Batch mode was where hydrogen was supplied in a syringe and data was collected in batches and results were tabulated. Whereas continuous mode is where the reaction was allowed to take place for long hours with no breaks.

Nanoparticle solutions of different acceptor-donor systems and compositions were prepared and used to run hydrogen evolution reactions. The results of each experiment are summarized below in *Table 3.3.*

Table 3.3: Represents the hydrogen evolution reaction result

Trails	Description	Hydrogen (µmol/h)	Hydrogen (µmol/g.h)
1	10:90 A1 NPs Batch	3.7	1848.3
2	10:90 A2 NPs Continuous	1.1	549.7
3	10:90 A2 NPs Batch	None	None
4	30:70 A1 NPs Batch	0.74	370.0
5	90:10 A1 NPs Batch	None	None
6	10:90 A2 NPs Batch, HPS water (no SA)	0.1	49.7
7	20:80 A1/D NPs Batch	0.05	27.2
8	30:70 A1/D film w/MoS2 Batch, no Pt	None	None
9	30:70 A1/D film w/MoS2 Batch	None	None
10	10:90 A1/D NPs w/MoS2 Batch	1.0	485.1
12	10:90 A1/D NPs Batch, lower Pt loading	0.7	328.1
13	10:90 A1/D NPs Batch	0.6	280.4
14	10:90 A3/D NPs Batch	3.6	-

The results clearly demonstrate that the A1/D and A3/D systems composed of a 10:90 A/D ratio provide the best results. The second NF-FREA variant, A2 resulted in significantly lower results, even at the optimum 10:90 A/D ratio. The results also demonstrate that the hydrogen evolution decreases as the acceptor amounts in the nanoparticles increase. This is shown by the 97% decrease in hydrogen production that is observed when the A1/D ratio is increased from a 10:90 A1/D ratio in experiment 1 to a 90:10 A1/D ratio in experiment 5. Additionally, platinum is observed to be the optimum co-catalyst since experiments 1 and 10 show a 73% decrease in hydrogen production when the co-catalyst is switched from platinum to molybdenum.

4. CONCLUSION

Polymeric photocatalysts are the solar cell materials of the future. Nature-inspired conjugated materials have been developed as a viable replacement for non-renewable resources. The solution of donors and acceptors resulted in higher bandgap energy compared to the films, this indicates that the solution of the nanoparticles had a smaller particle size. Hence, the solution of the nanoparticles would absorb light at a higher frequency and lower wavelength. However, the results demonstrate great potential for the use of organic catalysts in photocatalytic hydrogen production from water. The polymers NF-FREA1 and NF-FREA-3 showed the most promising results and need to be explored further. Different systems, surfactants, co-catalyst loadings, and reaction conditions can be explored to optimize the performance of the nanoparticles. The percentage of hydrogen evolution was demonstrated using different characterization techniques such as NMR and GC-mass spectrometer.

We were honored that our instructors had motivated us to work and participate in international and national conferences such as *International Conference on New Trends in Science and Applications* (NSTA), American Medical Student Association (ASMA) which is in collaboration with TAMU college station, and Qatar university online conference. The NTSA was held **virtually** via the zoom platform where we won 1st place in best poster design. The AMSA Research Symposium was held **virtually** via the Forager One where we participated by presenting our research poster with the results and data we have got. The Qatar university online conference was about Emerging and Enabling Materials that were held virtually via the Teams platform against multiple national and international universities. In addition, we have registered for the poster and presentation ACS research conference for chemistry and chemical engineering in MENA, which will be held on May 9-11, 2022 in Qatar.

REFERENCES

1. Xu, C.; Yang, Q.; Wang, F.; Fang, X.; Zhang, Z., Research progress on novel solar steam generation system based on black nanomaterials. *Canadian Journal of Chemical Engineering* **2018,** *96* (10), 2086-2099.

2. Kumari, S.; Turner White, R.; Kumar, B.; Spurgeon, J., Solar hydrogen production from seawater vapor electrolysis. *Energy and environmental science* **2016,** *9* (5), 1725-1733.

3. Takanabe, K., Photocatalytic Water Splitting: Quantitative Approaches toward Photocatalyst by Design. *ACS CATALYSIS* **2017,** *7* (11), 8006-8022.

4. Nocera, D. G., The artificial leaf. *Accounts of chemical research* **2012,** *45* (5), 767-776.

5. Chen, S.; Takata, T.; Domen, K., Particulate photocatalysts for overall water splitting. *Nature Reviews Materials* **2017,** *2* (10), 1-17.

6. Lewis, N. S.; Nocera, D. G., Powering the planet: Chemical challenges in solar energy utilization. *Proceedings of the National Academy of Sciences* **2006,** *103* (43), 15729-15735.

7. Hisatomi, T.; Kubota, J.; Domen, K., Recent advances in semiconductors for photocatalytic and photoelectrochemical water splitting. *Chemical Society Reviews* **2014,** *43* (22), 7520-7535.

8. Yang, J.; Wang, D.; Han, H.; Li, C., Roles of cocatalysts in photocatalysis and photoelectrocatalysis. *Accounts of chemical research* **2013,** *46* (8), 1900-1909.

9. Wang, H.; Li, W.; Liu, T.; Liu, X.; Hu, X., Thermodynamic analysis and optimization of photovoltaic/thermal hybrid hydrogen generation system based on complementary combination of photovoltaic cells and proton exchange membrane electrolyzer. *Energy conversion and management* **2019,** *183*, 97-108.

10. Sachs, M.; Sprick, R. S.; Pearce, D.; Hillman, S. A.; Monti, A.; Guilbert, A. A.; Brownbill, N. J.; Dimitrov, S.; Shi, X.; Blanc, F., Understanding structure-activity relationships in linear polymer photocatalysts for hydrogen evolution. *Nature communications* **2018,** *9* (1), 1-11.

11. Zhang, X.; Shen, F.; Hu, Z.; Wu, Y.; Tang, H.; Jia, J.; Wang, X.; Huang, F.; Cao, Y., Biomass nanomicelles assist conjugated polymers/Pt cocatalysts to achieve high photocatalytic hydrogen evolution. *ACS Sustainable Chemistry & Engineering* **2019,** *7* (4), 4128-4135.

12. Banerjee, T.; Lotsch, B. V., The wetter the better. *Nature chemistry* **2018,** *10* (12), 1175-1177.

13. Mikhnenko, O. V.; Blom, P. W.; Nguyen, T.-Q., Exciton diffusion in organic semiconductors. *Energy & Environmental Science* **2015,** *8* (7), 1867-1888.

14. Sun, C.; Wu, Z.; Hu, Z.; Xiao, J.; Zhao, W.; Li, H.-W.; Li, Q.-Y.; Tsang, S.-W.; Xu, Y.-X.; Zhang, K., Interface design for high-efficiency non-fullerene polymer solar cells. *Energy & Environmental Science* **2017,** *10* (8), 1784-1791.

15. Takanabe, K.; Kamata, K.; Wang, X.; Antonietti, M.; Kubota, J.; Domen, K., Photocatalytic hydrogen evolution on dye-sensitized mesoporous carbon nitride photocatalyst with magnesium phthalocyanine. *Physical Chemistry Chemical Physics* **2010,** *12* (40), 13020-13025.

16. Wang, X.; Chen, L.; Chong, S. Y.; Little, M. A.; Wu, Y.; Zhu, W. H.; Clowes, R.; Yan, Y.; Zwijnenburg, M. A.; Sprick, R. S.; Cooper, A. I., Sulfone-containing covalent organic frameworks for photocatalytic hydrogen evolution from water. *Nat Chem* **2018,** *10* (12), 1180-1189.

17. Richards, J. J.; Whittle, C. L.; Shao, G.; Pozzo, L. D., Correlating structure and photocurrent for composite semiconducting nanoparticles with contrast variation small-angle neutron scattering and photoconductive atomic force microscopy. *ACS nano* **2014,** *8* (5), 4313-4324.

18. Wang, L.; Fernández-Terán, R.; Zhang, L.; Fernandes, D. L.; Tian, L.; Chen, H.; Tian, H., Organic polymer dots as photocatalysts for visible light-driven hydrogen generation. *Angewandte Chemie* **2016,** *128* (40), 12494-12498.

19. Kosco, J.; Sachs, M.; Godin, R.; Kirkus, M.; Francas, L.; Bidwell, M.; Qureshi, M.; Anjum, D.; Durrant, J. R.; McCulloch, I., The effect of residual palladium catalyst contamination on the photocatalytic hydrogen evolution activity of conjugated polymers. *Advanced Energy Materials* **2018,** *8* (34), 1802181.

20. Liu, A.; Tai, C.-W.; Holá, K.; Tian, H., Hollow polymer dots: nature-mimicking architecture for efficient photocatalytic hydrogen evolution reaction. *Journal of Materials Chemistry A* **2019,** *7* (9), 4797-4803.

21. Kosco, J.; Bidwell, M.; Cha, H.; Martin, T.; Howells, C. T.; Sachs, M.; Anjum, D. H.; Gonzalez Lopez, S.; Zou, L.; Wadsworth, A.; Zhang, W.; Zhang, L.; Tellam, J.; Sougrat, R.; Laquai, F.; DeLongchamp, D. M.; Durrant, J. R.; McCulloch, I., Enhanced photocatalytic hydrogen evolution from organic semiconductor heterojunction nanoparticles. *Nat Mater* **2020,** *19* (5), 559-565.